Microstructure Characteristics of Unsaturated Compacted Scaly Clay

Camillo Airò Farulla and Marco Rosone

Abstract. Microstructure characteristics of unsaturated compacted scaly clay are investigated by MIP tests on freeze dried samples and observation of SEM photomicrographs. Effects of scale microstructure and increasing compaction stresses, and microstructure changes induced by loading and unloading paths and clay saturation are analysed.

Keywords: microstructure, compacted clay, wetting, loading, MIP tests.

1 Introduction

Extensive experimental studies have demonstrated the strong dependence of mechanical behaviour of tectonised clays on their structural arrangement characterised by different sets of discontinuities which subdivide the clays in tightly interlocked hard clayey fragments (scales). A wide evidence has been also collected on the influence that scales which survive compaction have on the mechanical properties of compacted scaly clays. In this respect, a better interpretation of the evolution of stiffness and shear strength of unsaturated compacted scaly clays, when subjected to complex suction and loading paths, could be obtained by a systematic analysis of microstructure evolution in consequence of stress paths applied.

Previous investigations have shown that at a microscopic level as-compacted scaly clays present an aggregated structure determined by scales and assemblages made of scale fragments and clay particle aggregations with different elementary

Camillo Airò Farulla
Università degli Studi di Palermo, Palermo, Italy
e-mail: camillo.airofarulla@unipa.it

Marco Rosone
Università degli Studi di Palermo, Palermo, Italy
e-mail: marco.rosone@unipa.it

particle arrangements. Scales are composed by very dense aggregates of oriented elementary particle arrangements (Airò Farulla & Jommi, 2005). The microstructure is characterised by a clear double porosity network, in which two principal levels can be identified: micropores inside assemblages and clay particle aggregations, and macropores between them (Airò Farulla et al., 2010).

The paper presents further data on the effects on microstructure of unsaturated compacted scaly clay of such factors as: scale microstructure, compaction effort, loading and unloading at constant suction, clay saturation and successive loading and unloading paths.

Microstructure was investigated by mercury intrusion porosimetry (MIP) tests along with observation of photomicrographs obtained by Scanning Electronic Microscope (SEM) on freeze dried samples (Romero & Simms, 2008).

2 Tested Material

Two different sample groups, named AC and B, were prepared using a stiff and highly fissured clay outcropping near Palermo (Sicily). It is a silty clay, with plasticity index $PI = 28 \div 30\%$, mean specific gravity $G_s = 2.76$, and natural water content $w_n = 20\%$.

The air dried clay was disaggregated by a rubber pestle and the material passing through a No. 10 ASTM sieve (mesh aperture of 2 mm) was selected for preparing samples AC. The selected material (composed mainly by sand-size clay fragments) was moistened to reach water content $w = 15\%$, and after a curing time of 2 or 3 days it was statically compacted into a small rigid cylindrical mould (inner diameter of 9 mm and height of 9.3 mm).

Samples B, subjected to wetting and/or loading-unloading paths by means of two oedometers were prepared by statically compacting ($\sigma_{vmax} \cong 1$ MPa) material passing through a No. 4 ASTM sieve (mesh aperture of 4.75 mm) after moistening to $w = 15\%$ (Airò Farulla et al., 2010). At the end of compaction values of void ratio, saturation degree and total suction, ψ, were: $e = 0.556 \div 0.577$, $S_r = 0.70 \div 0.75$, $\psi \cong 2$ MPa. Specimens for MIP tests and SEM observations were recovered from B samples at the end of the oedometer tests by means of a small cylindrical sampler (inner diameter of 10 mm and height of 10 mm).

3 Testing Equipment

MIP tests were performed using a porosimeter (Pascal 140-240 series, Thermo Scientific Corp.) attaining a maximum intrusion pressure of 200 MPa, which corresponds to an entrance pore diameter of 7.5 nm. Macropores were detected at the beginning of the tests in the low pressure unit operating between 0 and 400 kPa. The advancing non-wetting contact angle between mercury and the clay minerals was assumed to be 140° (Romero & Simms, 2008). SEM observations were performed on FEI Quanta 200f (maximum magnification 1000000X). MIP tests and

SEM observations were carried out on samples dehydrated by means of a freeze-drying technique consisting in quick freezing the samples by dipping them in liquid nitrogen (boiling temperature -198°C) and sublimation with vacuum pump at -60°C for 24 hours.

4 Experimental Programme

The MIP tests referred to in the paper were carried out on an intact stiff clay fragment (scale), on a group of three as-compacted scaly clay samples prepared with different initial unit dry weight (AC), and on three compacted samples subjected to different stress paths by means of two oedometers (B).

The scale (SC), drawn from an air dried clay sample, was moistened to a water content of about 14% by exposing it for a few days to a confined vapour saturated atmosphere at constant temperature ($T = 20° \pm 1°C$).

In order to evaluate microstructure evolution of the as-compacted material at increasing density, samples AC1, AC2, and AC3 were statically compressed at increasing stresses to achieve initial dry unit weight, γ_d, equal to 14, 16 and 18 kN/m^3, respectively.

Effects of applied stress paths on microstructure were investigated by tests carried out on the specimens B1, B2, B3 all prepared with initial $\gamma_d = 18$ kN/m^3 (like sample AC3). Sample B1 was subjected to a loading-unloading cycle in a suction controlled oedometer to maximum vertical net stress $\sigma_{vnet} = 1.6$ MPa at constant matric suction $s = 0.6$ MPa. Sample B2, was let swell in a conventional oedometer under applied vertical stress $\sigma_v = 10$ kPa (free or unconfined swelling). Specimen B3, after the initial saturation phase likewise sample B2, was subjected to a loading-unloading cycle to maximum applied vertical stress $\sigma_v = 6$ MPa.

5 Results Analysis

Results of MIP tests carried out on SC and AC samples are represented in the diagrams of Fig. 1 as cumulative intrusion pore volume of mercury normalized by solid volume ("intruded void ratio" e_i) (Fig. 1a) and pore size density ($PSD = -\delta e_i/\delta(\log D)$) (Fig. 1b) against pore entrance diameter D. With reference to the initial physical properties of the samples it is important to report that moistened scale presented void ratio $e_0 = 0.386$ and saturation degree $S_r = 0.97$. At the end of compaction values of void ratio and saturation degree of AC samples were: AC1: $e_0 = 0.959$, $S_r = 0.43$; AC2: $e_0 = 0.691$, $S_r = 0.60$; AC3: $e_0 = 0.533$, $S_r = 0.78$; measured total suction values were in the range $\psi = 2 \div 2.5$ MPa. Values of intruded e_i and measured void ratio e_0 of SC and AC samples are collected in Table 1.

Intact stiff clay (SC) begins to intrude at mercury pressure in the order of 1.5 MPa corresponding to a pore entrance diameter of about 1 μm. The PSD function shows a single porosity mode at $D = 0.09$ μm. The overall intruded void ratio is 0.241 lower than the initially measured void ratio $e_0 = 0.386$ (Table 1), in

consequence of the limited capacity of the porosimeter to enter the smallest pores and the entrapped pores.

Overall intruded void ratio, e_i, of the as-compacted clay samples AC decreases significantly as material density increases (Fig. 1a and Table 1). However, assuming a pore entrance diameter D =1 μm to separate micropore from macropore domains, micropore intruded void ratios (e_{micro}) fall in the narrow range 0.226 ÷ 0.247, while macropore intruded void ratios (e_{macro}) sharply decrease (from 0.319 to 0.153) as material dry density increases (Table 1). It can be argued that intruded void ratio decrements are mainly due to macropore volume reduction. The difference ($e_0 - e_i$) between measured and overall intruded void ratio increases as sample dry unit weight decreases, mainly because the non-detected largest pores are filled by mercury in the low pressure unit before test starting (Koliji et al., 2010).

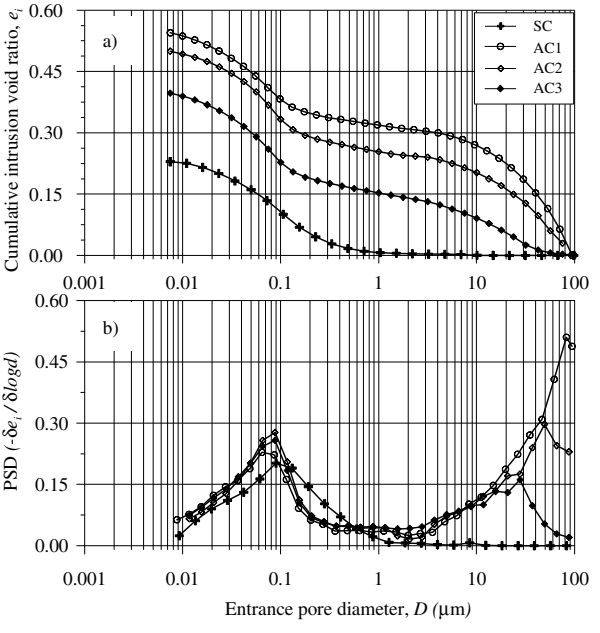

Fig. 1. Results of MIP tests on intact clay (SC) and as-compacted scaly clay (AC1-AC3, γ_d = 14 ÷ 18 kN/m^3).

The PSD functions (Fig. 1b) of the as-compacted scaly clay samples show a clear bimodal pore size distribution. The prevalent macropore entrance diameters decrease from 80 to 30 μm as γ_d increases from 14 to 18 kN/m^3, while the prevalent micropore diameters coincide with the prevalent diameter (0.09 μm) of the intact scale SC. It is evident from the diagrams in Fig.1 and the data collected in Table 1 that the scale and the as-compacted clay samples present only small differences as regarding to pore volume and PSD distributions for D < 1 μm.

It can be concluded that the fabric of aggregates is determined mainly by intact stiff clay (scale) microstructure.

The SEM photomicrograph of Fig. 3a highlights the structure of the as-compacted clay (sample AC3), characterised by large aggregates of particles and macrovoids between them. Micropores inside aggregates are not easily discernible at photomicrograph magnification.

Loading-unloading effects on microstructure characteristics of unsaturated compacted clay can be inferred by comparing results of MIP tests carried out on B1 and AC3 samples. Sample B1 was let equalize in a suction controlled oedometer to a net vertical stress σ_{vnet} = 50 kPa and matric suction s = 600 kPa, measuring a volumetric expansion strain ε_v = - 0.25%, and then subjected to a loading–unloading cycle (σ_{vnet} = 1.6 MPa). At the end of loading cycle a volumetric compression strain ε_v = 3.41% was measured and a final void ratio of 0.520 was calculated. Before freeze drying, void ratios, e_0, of AC3 and B1 samples are not very dissimilar: 0.533 and 0.520, respectively (Table 1). Compaction at constant matric suction induces only a small difference in the overall intruded void ratio, as e_i is 0.372 for B1 and 0.397 for AC3. However, macropore volume decreases significantly and e_{macro} reduces from 0.153 for AC3 to 0.090 for B1. Conversely, micropore volume for sample B1 increases as e_{micro} rises from 0.244 (AC3) to 0.283 (B1). Sample B1 retains a double porosity network, however its prevalent micropore diameter (D = 0.07 μm) is lower than the prevalent micropore diameter of sample AC3. Yet, in interpreting collected results it has to be considered that the stress path applied to sample B1 included a moderate matric suction reduction step before the loading cycle. In this respect, suction effects on pore size distribution may be considered as negligible because of the low intensity of applied suction reduction and induced material volumetric deformation (Monroy et al., 2007).

Table 1. Intruded (overall, e_i; macropore domain, e_{macro}; micropore domain, e_{micro}) and measured (e_0) void ratios.

Specimen	e_i	e_{macro}	e_{micro}	e_0	e_0 - e_i
SC	0.241	0.007	0.234	0.386	0.145
AC1	0.545	0.319	0.226	0.959	0.414
AC2	0.500	0.253	0.247	0.691	0.191
AC3	0.397	0.153	0.244	0.533	0.136
B1	0.372	0.090	0.283	0.520	0.148
B2	0.508	0.135	0.373	0.642	0.134
B3	0.357	0.027	0.330	0.520	0.163

On the contrary, saturation deeply modifies the microstructure of as-compacted scaly clay as shown by MIP test results relative to sample B2 (Fig. 2). Starting from the clear bimodal pore size distribution of the as-compacted clay samples (Fig.1), saturation leads to a prevalent monomodal pore size distribution with a sharp peak at D = 0.91 μm, even if a much more attenuate peak could be individuated at about D = 0.07 μm. Volume of macropores reduces significantly (e_{macro} = 0.135) and macropores with D > 10 μm almost disappear (Table 1; Fig. 2a).

On the contrary, micropore volume and PSD peak value of the prevalent diameter sharply increase (Table 1; Fig. 2b). The relevant increment of the overall intruded porosity in sample B2 is due to the micropore volume increment (Table 1).

Effects of saturation are well evident in the SEM photomicrograph of Fig. 3b: scale fragments and particle aggregations formed during compaction strongly expand invading macropores. Expanded aggregates are arranged in a very uniform pattern with very few macrovoids ($D = 5 \div 10$ μm) between them. Aggregates are still discernible as distinct units.

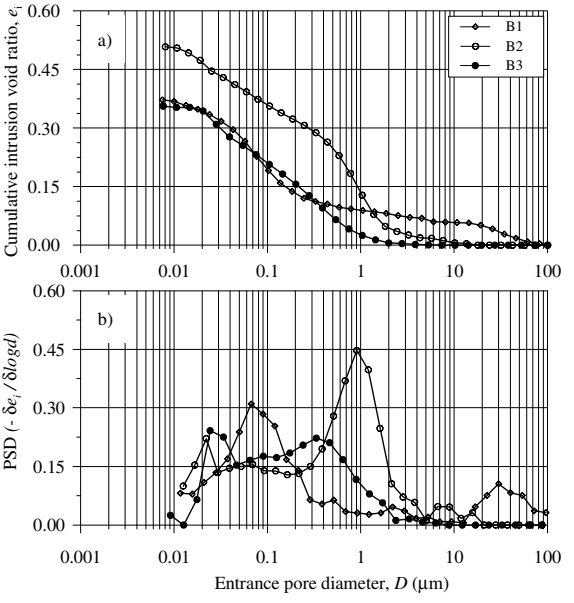

Fig. 2. Results of MIP tests on B1, B2 and B3 samples.

During saturation sample B2 swelled accumulating an overall volumetric expansion strain ε_v = - 4.1 % and increasing void ratio from 0.577 (as-compacted condition) to 0.642 (referred as e_0 in Table 1). Volumetric expansion induced by suction reduction is due to the high density of the as-compacted material (γ_d = 18 kN/m^3) and the low total vertical stress applied. At a microscopic level, material swelling is the consequence of the expansion of scales and clay particle aggregation. Indeed, MIP test results (Fig. 2a,b) and photomicrograph in Fig. 3b indicate that both volume and size of inter-aggregate macropores reduce significantly in consequence of saturation. It is also of interest to underline that at saturation the prevalent pore diameter D = 0.91 μm is very near to the diameter assumed to separate micro and macro pore domains (Della Vecchia, 2009; Cardoso & Alonso, 2010).

The effects of compaction on the microstructrure of saturated compacted scaly clay can be detected by comparing results of tests on B2 and B3 samples. During

unconfined saturation B3 experienced a volumetric swelling strain ε_v = - 6.0 %, achieving at equilibrium a void ratio of 0.669. The loading-unloading cycle (σ_{vmax} = 6 MPa) induced a total volumetric compression strain ε_v = 2.4% , with a corresponding void ratio e_0 = 0.520 (Table 1). The results of B3 test show that the loading-unloading cycle reduces intruded void ratio of the saturated material from 0.508 to 0.357 essentially as consequence of the reduction of macropore volume which almost disappears (e_{macro} = 0.027) (Table 1). The PSD function of sample B3 retains a monomodal distribution, but in comparison with PSD of B2 it is shifted to the left (micropore dominium) and both values of prevalent pore diameter and peak PSD reduce greatly (Fig. 2b). However, for D < 0.05 μm intruded void ratio and PSD function of saturated compacted clay before (B2) and after loading-unloading cycle (B3) are very similar.

The dependence of aggregated soil structure on stress paths applied can be illustrated by considering results of tests carried out on B1 and B3 samples. As evident from the data collected in Table 1, the samples have the same measured void ratio (e_0 = 0.520) and their overall intruded void ratios are not very different: 0.372 for B1 and 0.357 for B3 (Fig. 2a). However their PSD functions are characterised by some significant differences. Sample B1 retains some macropore volume (e_{macro} = 0.090) and presents a sharp PSD peak (0.30) for D = 0.07 μm. Sample B3 presents a greater intrude volume in the micropore domain and a more uniform micropore diameter distribution. As a matter of fact densities of pore entrance diameter in the range 0.03 ÷03 μm share very similar values (0.18÷0.21).

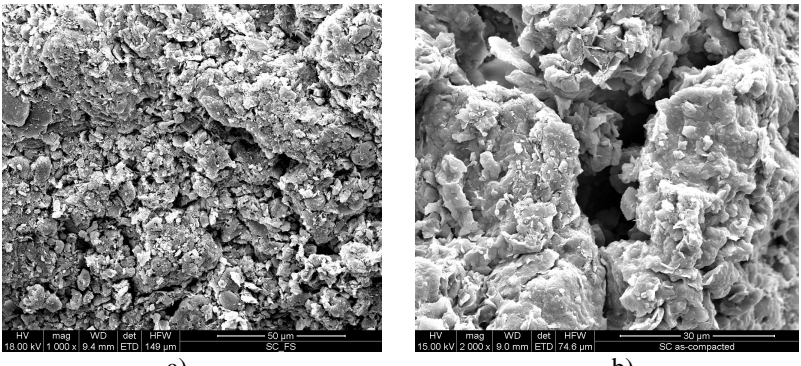

a) b)

Fig. 3. SEM photomicrographs on freeze-dried samples: a) as-compacted scaly clay (γ_d = 18.0 kN/m^3); b) compacted scaly clay saturated under free swelling conditions.

6 Conclusions

Analysis of the data presented in the paper enables to state that the microstructure of as-compacted scaly clay depends mainly on the microstructure of intact stiff clay fragments (scales) which survive compaction irrespective of the intensity of

compaction stress. Pore volume reduction induced by increasing material dry density derives from the inter-aggregate pore volume reduction, while intruded volume and PSD function of intra-aggregate pores remain constant even if compaction stress is strongly increased. Besides, they present only minor differences respect to intruded volume and PSD distribution in the micropore domain of intact stiff clay.

A loading and unloading cycle at constant suction of unsaturated as-compacted scaly clay reduces overall intruded void ratio mainly by a corresponding reduction of macropore volume.

Saturation is able to deeply change the microstructure of the compacted scaly clay modifying the double porosity network of the as-compacted material in a prevalent mono-modal pore diameter distribution. Suction reduction in oedometer under a low confinement stress induces a very high expansive volumetric strain as consequence of expansion of scale fragments and particle aggregations formed during compression. Aggregates expand invading macropore volume which strongly reduces. As a consequence, volume of micropores and their prevalent diameter density sharply increase.

The data presented in the paper contribute to give further evidence of some characteristic effects of stress paths applied, and suction reduction in particular, on the microstructure of clayey soils with an aggregated structure as well documented in previous research works. They also evidence the peculiar influence that the presence of stiff clay fragments exercises upon the behaviour of compacted scaly clays.

References

Airò Farulla, C., Ferrari, A., Romero, E.: Volume change behaviour of a compacted scaly clay during cyclic suction changes. Can. Geotech. J. 47, 688–703 (2010), doi:10.1139/T09-138

Airò Farulla, C., Jommi, C.: Suction controlled wetting drying cycles on a compacted scaly clay. In: Proc. of Int. Conf. on Problematic Soils, vol. 1, pp. 229–238 (2005)

Cardoso, R., Alonso, E.: Structural changes of compacted marls subjected to suction cycles. In: Buzzi, F., Sheng (eds.) Proc. South East Asiatic Conference on Unsaturated Soils, pp. 83–88 (2010)

Della Vecchia, G.: Hydro-mechanical coupled behaviour of compacted clayey soil. PhD thesis, Politecnico di Milano (2009)

Koliji, A., Vulliet, L., Laloui, L.: Structural characterization of unsaturated aggregated soil. Can. Geotech. J. 47, 297–311 (2010), doi:10.1139/T09-089

Monroy, R., Zdravkovic, L., Ridley, A.: Fabric changes in compacted London Clay due to variations in applied stress and suction. In: Schanz, T. (ed.) Experimental Unsaturated Soil Mechanics, pp. 41–47. Springer, Heildelberg (2007)

Romero, E., Simms, P.H.: Microstructure investigation in unsaturated soils: a review with special attention to contribution of mercury intrusion porosimetry and environmental scanning electron microscopy. Geotechnical and Geological Engineering 26, 705–727 (2008), doi:10.1007/s10706-008-9204-5